Published in final edited form as:
J Am Chem Soc. 2006 July 26; 128(29): 9387–9393. doi:10.1021/ja057693+.

Direct Detection of the Formation of V-Amylose Helix by Single Molecule Force Spectroscopy

Qingmin Zhang[†], **Zhenyu Lu**[§], **Hao Hu**[§], **Weitao Yang**[§,*], and **Piotr E Marszalek**[†,*]

† *Center for Biologically Inspired Materials and Material Systems, and Department of Mechanical Engineering and Materials Science, Duke University, Durham, NC 27708*

§ *Department of Chemistry, Duke University, Durham, NC 27708*

Abstract

An important polysaccharide, amylose crystallizes as a regular single left-handed helix from a propanol, butanol or iodine solution. However, its solution structure remains elusive because amylose does not form molecular solutions in these solvents, and standard spectroscopic techniques cannot be exploited to determine its structure. Using the AFM, we forced individual amylose chains adsorbed to a surface to enter these poor solvents and carried out stretch-release measurements on them in solution. In this way, we directly captured the formation of individual amylose helices induced by butanol and iodine. With an accuracy approaching that of X-ray diffraction on amylose crystals, we determined that the pitch of the helix in solution is 1.3 Å/ring. We also directly measured the force driving the formation of the helix in solution to be 50 pN. SMD simulations in explicit butanol reproduced the AFM-measured force-extension curves and revealed that the long plateau feature is caused by the rupture of $O(2)_n$-$O(6)_{n+6}$ and $O(3)_n$-$O(6)_{n+6}$ hydrogen bonds and by the unwinding of the helix. We also found that amylose helices formed in iodine solution are more compliant and hysteretic as compared to helices in butanol, which extend/relax reversibly. In iodine solution, the formation of the helix is inhibited by force and limited by the slow kinetics of the amylose-iodine complex. By forcing individual molecules into poor solvents and performing force spectroscopy measurements in solution, our AFM approach uniquely supplements X-ray diffraction and NMR methods for investigating solution conformations of insoluble biopolymers.

Introduction

In neutral aqueous solutions, amylose, a linear 1→4 linked α-D-glucan and the principal component of starch, behaves as a flexible random coil that contains randomly distributed stretches of short helical segments.[1] On the other hand, the amylose that crystallizes from aqueous iodine solutions, butanol or pentanol reveals very regular structures called V-amylose complexes, which have been characterized as left-handed single-stranded helices that contain six glucose residues per turn[2–4] with a pitch of 7.8 Å (butanol wet precipitates) and 7.9 Å (iodine crystals).[5,6] Structural studies on these complexes indicate that polyiodine and butanol molecules fill the helical cavity of amylose.[5–7] However, in spite of much effort, the *solution* structure of amylose in these complexes has remained elusive.[8]

Recent force spectroscopy measurements of various polysaccharides performed with the atomic force microscope (AFM) have revealed that relatively simple mechanical manipulations can be very informative in probing molecular conformations in solution. For example, by mechanically stretching single amylose or dextran molecules, it becomes possible to force all

Email: weitao.yang@duke.edu; pemar@duke.edu.

the constituent sugar rings in a polysaccharide chain into high energy conformations such as boat-like structures. Thus, force spectroscopy makes it possible to investigate ring conformations, which normally are not accessible to other structural methods because these methods can only study molecules in or near equilibrium.[9–14] Similar AFM studies found unique elastic fingerprints of multi-helical polysaccharide structures of curdlan, carrageenan and xanthan and differentiated between ordered and random coil structures.[15–17] An interesting and unique feature of single molecule force spectroscopy is that the AFM cantilever can pull macromolecules into solvents in which these molecules normally do not dissolve. Such experiments, then, can reveal the solution behavior of "insoluble" molecules. For example, this type of molecular manipulation has already enabled direct measurement of intra-molecular hydrogen bonds in amylose that had been pulled into the poor solvent dimethyl carbonate.[18]

Here, we use AFM-based single-molecule force spectroscopy to pull individual amylose molecules into aqueous iodine solution and into butanol to directly probe the relationship between their mechanical properties and their secondary structure in these solvents. We corroborate our results by steered molecular dynamics simulations of amylose in explicit butanol. Our force spectroscopy measurements provide a new means to study polymer structures in a variety of environments, including poor solvents, for which other spectroscopic methods cannot be used.

Materials and Methods

AFM-based single-molecule force spectroscopy

Force spectroscopy measurements were carried out on a homemade single-axis AFM instrument. This force spectrometer was equipped with an AFM detector head from the MultiMode AFM (Veeco, USA) and a piezoelectric actuator with an integrated strain gauge for direct measurements of the travel of the piezo (open-loop travel resolution of 0.15 nm; Physik Instrumente, Germany). The instrument was controlled by a PC computer using a 16 bit A/D-D/A interface (National Instruments). The spring constant of each Si_3N_4 cantilever (Veeco) was calibrated using the energy equipartition theorem as described in reference [19].

Polysaccharides

Amylose was obtained from Sigma-Aldrich (Type III from potato). Butanol was obtained from Mallinckrodt Co. Iodine aqueous solution was made from iodine (Sigma) and KI (Sigma) with a concentration of 0.04 % and 0.2 %, respectively. This solution was then diluted 4 times to 0.01 % of iodine and 0.05 % of KI. Amylose triacetate (ATA) was kindly provided by Prof. Yasuhiro Takahashi of Osaka University, Japan.

Amylose was dissolved in water at a concentration of 0.02 % by heating. To adsorb amylose molecules onto a glass substrate, a drop of amylose aqueous solution (~40 μL) at a concentration of 0.02 % w/v was placed on the glass surface for several hours and allowed to dry. The dehydrated sample was rinsed several times with water to remove most of the molecules and leave only those that had tightly adsorbed to the substrate. The sample, mounted on a metal disk, was placed in the AFM instrument, and the fluid chamber was filled with the proper liquid, a pure butanol or iodine aqueous solution. To pick up single amylose molecules, the AFM tip was pressed against the substrate at a force of 1–40 nN and subsequently withdrawn.

Normalization of force spectrograms

In order to verify that a given recording was obtained on a single molecule, it is necessary to compare it with a set of consistent single-molecule force spectrograms. Because the AFM tip

picks up molecular fragments randomly with respect to their ends, the stretched fragments are of widely different lengths. Thus, to compare different recordings, it is necessary to normalize the molecule's extension. This procedure, based on the properties of the freely-jointed-chain (FJC) model of polymer elasticity, is described in detail in our previous papers.[12,18] In addition, to express the normalized chain extension per sugar ring, we exploited the results of steered molecular dynamics simulations of the stretching of amylose. Such simulations established that the amylose extension per glucose ring at a force of 3270 pN is 5.57 Å, and this length is independent of the solvent.[18] To normalize the experimental force curves, therefore, we assume that the extension of these chains "per ring" is at 3270 pN equal to 5.57 Å. To normalize force curves that did not reach 3270 pN, we simply used the curves that reached 3270 pN as templates to give the "correct" lengths at lower forces.[18] This procedure established that in water, the normalized extension of the amylose chain at a force of, e.g., 1170 pN is 5.265 Å/ring (see Figure 1a)(for details, see Supporting Information).

Molecular Dynamics Simulations

An amylose fragment of 18 glucopyranose rings was built with the CHARMM program.[20] To generate the helical structure as found in the amylose crystal,[6] the amylose fragment was subjected to a 1 ns restraint-applied MD simulation, in which the distances between the mass centers of every other six glucopyranose rings were restrained to 8.0 Å. The generated helical structure of the amylose fragment was then solvated by a butanol or water box. To prevent the helical structure from being distorted by the solvent molecules, 1 ns MD simulations with the position restraints on the solute (amylose fragment) were performed.

To simulate the AFM experiment, steered molecular dynamics (SMD) and constant force simulations were performed. In the SMD simulation, the O(1) atom of the reducing end (residue 18) was fixed, while the O(4) atom of the nonreducing end (residue 1) was subjected to a time-dependent spring force,

$$F_{spring}=k_{cant}[z_{cant}(t)-z_{O4}(t)]$$

where z_{cant} and z_{o4} are the coordinates (projected on the pulling direction) of the cantilever and the O(4) atom of the first glucopyranose ring. The cantilever moved with a constant velocity v_{cant}. A total of 24 ns SMD simulation was performed with the spring force constant k_{cant}=0.1 kcal/mol·Å^2 and the cantilever velocity v_{cant}=0.01 Å/ps. In the constant force simulations, the O(1) atom of the reducing end of the amylose was fixed, and the O(4) atom of the nonreducing end was subjected to a constant stretching force.

The OPLS force field[21,22] was used for the SMD and constant force simulations. Several additional MD simulations were performed with the CSFF[23] and GLYCAM04[24–26] force fields for amylose and a CHARMM force field[27] for butanol. Without further notes, all the molecular dynamics simulations were performed in the NVT ensemble with the NAMD program.[28] The box size is 120 × 60 × 60 Å^3 in the SMD simulation and 60 × 60 × 60 Å^3 in the rest of the simulations. The time step was 2 fs, and all bonds involving hydrogen atoms were fixed. The short-range nonbonded interactions were calculated with a cutoff of 12 Å, and the nonbonded pairlist was updated every 20 steps with a cutoff of 16 Å. The long range electrostatic interactions were computed with the Particle Mesh Ewald (PME) method.[29] All the simulations were done at a constant temperature of 300 K.

Results and Discussion

The elastic properties of amylose in butanol

To characterize the mechanical properties of amylose molecules in butanol, we picked them up individually from the glass surface with the AFM tip, stretched vertically, and then relaxed. Figure 1a shows two normalized force-extension relationships obtained on stretching (green curve) and relaxing (red curve) a single amylose chain in butanol. In water, amylose stretching occurs with minimal force, and f≈0 until ~80 % of the contour length is reached (Figure 1a, gray trace). In contrast, the initial stretching of amylose in butanol (Figure 1a, green trace) requires a significant force of ~50 pN, producing a long plateau in the force-extension curve that starts almost at the onset of the stretching and ends at the extension of ~3.4 Å/ring. This observation immediately suggests that in butanol, amylose does not behave as a purely entropic coil but displays a significant intrinsic (enthalpic) elasticity. In addition, unlike in water, in butanol the stretching and relaxing curves do not fully overlap but reveal a certain amount of hysteresis. Interestingly, the relaxing trace also reveals a long plateau at 50 pN that abruptly ends at the extension of 1.3 Å/ring, with the force falling to near zero in a step-wise fashion (Figure 1a, red trace). Such an elastic behavior with a pronounced plateau feature is reminiscent of the plateaus observed for other polysaccharides such as xanthan[17] and curdlan[15] and also for the double-stranded DNA.[30, 31] In each of these cases, the plateau was attributed to the conformational transition of helices from their compact state to the extended state (triple helices in xanthan and curdlan and the double helix in DNA). Thus, it is tempting to hypothesize that the amylose plateau also reflects the elasticity of a helix. The reason why the stretching trace does not display a zero-force baseline as in the relaxing trace is not entirely clear. It is probably related to the fact that at the beginning of the stretch in a poor solvent, amylose must be desorbed from the glass and forced into the solution phase, which requires a finite force. These effects do not occur during the relaxing part of the measurement because the molecule remains in solution above the substrate most of the time and contacts the substrate only after the formation of the helix is completed.

V-Amylose helix

To further investigate the properties of these putative helices, we compared a number of *relaxing* force curves obtained on amylose molecules with different lengths (Figure 1b). All these curves reveal a similar plateau feature, and, when normalized and superimposed, these recordings overlap very well, proving that the length of the plateau is proportional to the molecule length (Figure 1c). In addition, the force-steps that end the plateau feature in each case occur at the characteristic extension of 1.3 Å/ring. We hypothesize that when the pre-stretched amylose chain is allowed to relax, the helical turns are formed, generating a constant force (Figure 1c, inset). This helix formation is finished when the normalized extension decreases to ~1.3 Å/ring. Then the helix behaves as a rigid rod that generates a minimal entropic tension, and, therefore, the force measured by the AFM cantilever drops to ~zero in a step-wise fashion.

It is illuminating to examine the dimensions of the amylose helix established by X-Ray diffraction measurements of butanol-precipitated amylose.[5] These studies indicate that the pitch of the amylose helix is 7.8 Å and that each helical turn is composed of six glucopyranose rings. Thus, X-ray measurements indicate that the length along the helix axis per one sugar ring is 1.3 Å. It is significant that our simple stretch and release measurements give exactly the same length of amylose per ring at the end of the plateau feature, strongly suggesting that at this characteristic force-step, the amylose chain has assumed a compact helical structure that is similar to the one found in amylose crystals. This observation also suggests that amylose helices formed in the solution phase must be very similar to those that produce diffraction patterns from closely packed structures formed in butanol precipitates. We consider the

agreement between our simple mechanical measurements and X-ray studies to be quite remarkable, pointing to unprecedented possibilities of AFM-based force spectroscopy to characterize molecules' conformations in solution that might complement X-ray studies of crystals.

According to previous structural studies, the glucose rings of V-amylose are all in *syn* orientation. Consequently, the inter-glucose hydrogen bond $O(3)_n$-$O(2)_{n+1}$ and the inter-turn hydrogen bonds $O(2)_n$-$O(6)_{n+6}$ and $O(3)_n$-$O(6)_{n+6}$ are formed and stabilize the helix structure (Figure 1a inset).[6] Thus, it is likely that a force of ~50 pN is needed to sequentially break these bonds upon stretching the amylose helix. It is interesting that this force is similar to the force that is required to overstretch the helices of curdlan or double-stranded DNA (60–65 pN) by breaking their intra-molecular hydrogen bonds.[15, 31] It is significant that an identical force of 50 pN is generated by amylose upon relaxing its chain during the plateau feature. This 50 pN force must be driving the formation of the V-amylose helix.

We note that our typical AFM measurements of amylose in butanol were carried out within a narrow range of extension and retraction rates of 0.3 to 0.6 nm/ms. Conformational transitions in biopolymers were shown to depend on the extension rate, as has been well-documented for the forced unfolding of protein domains.[32] Thus, it is plausible that the magnitude of the force necessary to break the amylose helix, as well as the force generated upon its formation, may also depend on the rate at which the amylose chain is stretched and relaxed. We extended the range of stretching/retracting rates to ~0.1–2 nm/ms but found that the plateau force was not significantly affected at the lowest and the highest rates (after considering the hydrodynamic effect on the cantilever at higher extension rates) (for details, see Supporting Information). From these additional experiments, we conclude that 50 pN is a reasonable estimate of the magnitude of the force that is necessary to break the V-amylose helix in butanol and is generated by the amylose chain when it forms and contracts the turns of the V-helix.

Molecular dynamics simulations of amylose in the explicit butanol solvent

Computational methods have significantly contributed to the investigation of conformations of amylose and glucose rings[24, 33, 34] and molecular dynamics approaches have proved invaluable in aiding the interpretation of AFM measurements.[18, 35–37] Using the OPLS force field, we performed MD simulations of amylose in butanol and water. We found that although the V-Amylose helix was unfolded during the initial stage of the MD equilibration in water (see Fig. S4), it was well maintained during the 2 ns MD equilibration in butanol. As illustrated in Figure 2a, the averaged distance between every other six rings computed from the trajectory was about 8.2 ± 0.8 Å, which is consistent with X-ray measurements of the pitch of V-Amylose helix.[6] When examining the equilibration trajectory, we observed a network of hydrogen bonds, $O(2)_n$-$O(6)_{n+6}$ and $O(3)_n$-$O(6)_{n+6}$, which stabilized the helical structure. We also found that three butanol molecules penetrated the central channel of the amylose helix and stayed there during the whole equilibration time, apparently providing additional stabilization to the helix. To validate the results from the OPLS force field simulations, additional MD simulations were performed using the CSFF force field and the GLYCAM04 force field. As shown in Fig. S4, consistent with the results from the OPLS force field simulation, the averaged distance between every other six rings fluctuates around 8 Å during the GLYCAM04 MD simulation. The average distance from the CSFF simulation is higher (~9 Å), but the trajectory shows that the central part of the amylose chain is still forming V-Amylose helix.

To clarify the nanomechanical properties of the amylose helix in butanol, we carried out SMD simulations of stretching the amylose fragment in the explicit butanol solvent. The simulated force-extension curve of amylose is shown in Figure 2b, and the typical structures during different phases of the pulling process are displayed as insets. We see that at the normalized extension of 1.45 Å the force increases to ~100 pN, and this event is followed by a short plateau

from 1.5 – 2.0 Å. The SMD trajectory revealed that this short plateau comes from the breakup of the helical structure at the nonreducing end of the amylose chain. This is manifested by the increase in distances between $O(2)_n$ or $O(3)_n$ and $O(6)_{n+6}$, n=1,2,3 (see Figure 2c for an example), which indicates the rupture of hydrogen bonds between every other six sugar rings at the nonreducing end. Breaking the rest of the tight helical structure required even greater forces because at the extension of 1.95 Å the force increased step-wise to 200 pN, and this event started the long plateau feature in the force-extension curve. As indicated in Figure 2d, the last hydrogen bonding that ruptured during the plateau phase at an extension of 3.1 Å was that between $O(3)_{10}$ and $O(6)_{16}$. Interestingly, the pitch of the helix did not increase evenly along the helix during the stretch. The breakup of the helical structure propagated from the nonreducing end to which the pulling force was attached to the reducing end, which was kept fixed. At extensions greater than 4.6 Å, the pulling force was large enough to trigger the chair-to-boat transitions of individual sugar rings.[9] This phenomenon is consistent with our previous simulation of amylose in water.[35] At the end of this simulation (f=1200 pN), 14 out of 18 monomers were in a boat-like conformation (Figure 2b, inset). We note that the SMD simulation overestimated the forces necessary to break the helix as compared to AFM measurement. To obtain a more accurate measurement of the unfolding force from the simulations, we performed two constant force MD simulations, with the stretching forces equal to 20.85 pN and 41.70 pN, respectively. As manifested by the averaged distances between every other six rings (see Fig. S3), although the V-Amylose helix structure is stable in the 20.85 pN constant force simulation, the helical structure is unfolded in the 41.70 pN constant force simulation. Therefore, the constant force simulations suggest that a force of 41.70 pN or lower can break the V-Amylose helix in butanol. Although our MD simulations only yield qualitative agreement with the AFM experimental data, they still provide new insights into the behavior of the amylose butanol complex in equilibrium and capture the essential features of the AFM measurement.

Amylose Triacetate (ATA)

To further test the role of hydrogen bonds in the amylose helix formation in butanol, we examined the elastic properties of ATA, [38] in which the hydroxyl groups of glucose are replaced with acetate groups. These substitutions abolish the ability of glucose to form inter-residue hydrogen bonds (Figure 3, inset). In Figure 3, we compare the relaxing force curves of ATA in butanol (black curve) and in water (cyan curve). It is evident that the long plateau feature is not present in these curves. In addition, the curves are very similar to each other, suggesting that once the ability to form H-bonds has been eliminated, the effect of butanol on amylose elasticity is not significant.[18] Moreover, the shape of the ATA force curves, with a prominent transition feature at ~280 pN at higher extensions > 4.0 Å/ring, is similar to the shape of the force curves obtained on *unsubstituted* amylose in water (cf. Figure 1a, gray curve). Thus, our results on ATA support the conjecture that intra-molecular hydrogen bonds are important in forming a tightly coiled amylose helix in butanol.

Amylose elasticity in aqueous iodine solution

The interaction between iodine and amylose has been studied for many years because of iodine's intriguing ability to detect starch in solution by staining it with a characteristic blue color.[39] It is thought that the amylose-iodine complex has almost the same helical structure as the amylose-butanol complex, namely, V-amylose with six glucose rings per turn, with the polyiodine occupying the interior of the helix both in crystals[2, 5, 7, 40, 41] and in dissolved complexes.[5,7] With the AFM, we probed the mechanical properties of individual amylose molecules in aqueous iodine solution, and Figure 4a shows examples of the force-extension curves obtained upon stretching and relaxing the molecules. We note, first, that the stretching and relaxing traces show a long baseline of ~zero force, and neither clearly displays the long plateau feature that was so pronounced in butanol. Second, unlike in pure water, the relaxing

traces do not overlap with the stretching traces, revealing a significant hysteresis. Third, after extension normalization, all the stretching traces overlap well among themselves, as do the relaxing traces (Figure 4a inset). Fourth, the force curves reveal a transition at ~280 pN, which is also characteristic of amylose in pure water, where it was found to signal chair-boat transitions of the glucopyranose rings.[9] Fifth, at extensions greater than 4.5 Å/ring, the normalized *relaxing* traces overlap well with the force curves obtained in pure water (cf. red and green curves in Figure 4b). Sixth, at extensions between 4.0 and 4.5 Å/ring these force-curves run slightly below the force-curve measured in pure water, suggesting that the mutual orientation of the sugar rings (the configuration of the amylose chain) in the presence of iodine is slightly different than the one in pure water. At extensions lower than 4.0 Å/ring, the relaxing force-curves in iodine solution run above those obtained in pure water. This last observation likely suggests the presence of intra-molecular helix-forming forces that, however, are significantly weaker than in butanol.

The pronounced hysteresis between the stretching and relaxing behavior of amylose in iodine solution suggests that iodine significantly modifies the secondary structure of amylose as compared to pure water, where no hysteresis is observed.[9] It seems that after the helix has been fully stretched and the iodine molecules lose their close association with amylose, its elasticity becomes similar to the elasticity measured in pure water (Figure 4b). Consistent with the fairly long half-time of the amylose-iodine reaction, estimated at 0.4 s,[42] the hysteresis between the stretching and relaxing force curves indicates that the unraveled amylose does not re-form the helical structure immediately and also points to the inability of iodine to organize the helical turns when amylose is subjected to tensile forces. However, the formation of the helix in iodine solution probably starts when the amylose extension decreases below ~4 Å/ring, because at these lower extensions the force-extension curves start to run above the curves measured in pure water.

To further investigate the formation of the amylose helix in aqueous iodine solution, we carried out an experiment in which amylose molecules, after being stretched, were only partially relaxed to various initial lengths and these states were the starting points for subsequent stretching and relaxing measurements. The results are shown in Figure 5. It is evident that the amount of hysteresis in these recordings is directly related to the extent of relaxation of the amylose chain. When the chain was partially relaxed to only 3.2 Å/ring, the hysteresis between the subsequent stretching and relaxing force curves was barely noticeable. As in the previous measurements, all the relaxing traces overlapped well (Figure 5 inset), suggesting that they do not depend on the stretching history. Thus, we conclude that the magnitude of this hysteresis directly reflects the extent of the ordered helical structure that formed upon relaxing the amylose chain.

A comparison of amylose helices in butanol and in iodine solution

Our mechanical manipulations on single amylose molecules indicate that, in butanol and iodine solutions, amylose forms secondary structures that are likely to be V-amylose helices. In butanol, this is indicated by the long plateau feature at 50 pN in the relaxing force curve, which leads to the formation of a structure with a pitch of 1.3 Å/ring. In iodine solution, the existence of the helix is supported by a large hysteresis between stretching and relaxing traces. This hysteresis indicates amylose's secondary structure in the relaxed state, which is quasi-irreversibly destroyed upon stretching. The fact that in iodine solutions relaxing measurements do not produce a pronounced plateau, but only a slightly risen and sloped force baseline, indicates that the helix-forming intra-molecular forces are significantly weaker than in butanol. This difference can be attributed to the difference in the strength of intra-amylose hydrogen bonds, which are fairly strong in butanol (low dielectric constant of ε=17.8) and weak in aqueous solutions (high dielectric constant, ε=80). As suggested by the SMD simulation, the

stretching of the amylose helix through the plateau feature involves breaking the intra-turn hydrogen bonds $O(2)_n$-$O(6)_{n+6}$ and $O(3)_n$-$O(6)_{n+6}$, which, in AFM measurements requires a force of ~50 pN. The $O(3)_n$-$O(2)_{n+1}$ bonds are probably still preserved in butanol, even at extensions greater than 4 Å/ring, and their presence is responsible for the deviation of the force curve from that measured in pure water.[18]

Conclusions

Our AFM elasticity measurements captured the formation of compact amylose helices in butanol. We directly measured the helix pitch and the force driving helix formation. The results suggest that similar amylose helices are formed in iodine solution. These measurements are corroborated by molecular dynamics calculations in the explicit butanol solvent. Because the length of the relaxed amylose helix per glucose ring measured by AFM agrees so well with the length obtained from X-ray diffraction studies of crystals, we believe that single-molecule force spectroscopy can complement X-ray diffraction methods and is uniquely suited for investigating solution conformations of polysaccharides in good and poor solvents for which other spectroscopic methods cannot be used.

Acknowledgements

This work was supported by a grant from the National Science Foundation and by Duke University funds to PEM and by a grant from the National Institutes of Health to WY. We are grateful to Prof. Yasuhiro Takahashi of Osaka University, Japan, for a sample of amylose triacetate.

References

1. Robyt, JF. Essentials of Carbohydrate Chemistry. Springer-Verlag; New York: 1998. p. 163
2. Helbert W, Chanzy H. Int J Bio Macromol 1994;16:207–213. [PubMed: 7848968]
3. Bail PL, Rondeau C, Buleon A. Int J Bio Macromol 2005;35:1–7. [PubMed: 15769508]
4. Rappenecker G, Zugenmaier P. Carbonhydr Res 1981;89:11–19.
5. Rundle RE, Edwards FC. J Am Chem Soc 1943;65:2200–2203.
6. Gessler K, Uson I, Takahai T, Krauss N, Smith SM, Okada S, Sheldrick GM, Saenger WS. Proc Natl Acad Sci USA 1999;96:4246–4251. [PubMed: 10200247]
7. Rundle RE, Baldwin RR. J Am Chem Soc 1943;65:554–558.
8. Hirai T, Hirai M, Hayashi S, Ueki T. Macromol 1992;25:6699–6702.
9. Marszalek PE, Oberhauser AF, Pang YP, Fernandez JM. Nature 1998;396:661–664. [PubMed: 9872313]
10. Marszalek PE, Oberhauser AF, Li H, Fernandez JM. Biophys J 2003;85:2696–2754. [PubMed: 14507732]
11. Marszalek PE, Pang YP, Li H, Yazal JE, Oberhauser AF, Fernandez JM. Proc Natl Acad Sci USA 1999;96:7894–7898. [PubMed: 10393918]
12. Marszalek PE, Li H, Fernandez JM. Nat Biotech 2001;19:258–262.
13. Li H, Rief M, Oesterhelt F, Gaub HE, Zhang X, Shen J. Chem Phys Lett 1999;305:197–201.
14. Rief M, Oesterhelt F, Heymann B, Gaub HE. Science 1997;275:1295–1297. [PubMed: 9036852]
15. Zhang L, Wang C, Wang Z, Zhang X. Nano Lett 2003;3:1119–1124.
16. Xu QB, Zou S, Zhang WK, Zhang X. Macromol Rapid Commun 2001;22:1163–1167.
17. Li H, Rief M, Oesterhelt F, Gaub HE. Adv Mater 1998;10:316–319.
18. Zhang Q, Jaroniec J, Lee G, Marszalek PE. Angew Chem Int Ed 2005;44:723–2727.
19. Florin EL, Rief M, Lehmann H, Ludwig M, Dornmair C, Moy VT, Gaub HE. Biosens Biolelectr 1995;10:895–901.
20. Brooks BR, Bruccoleri RE, Olafson BD, States DJ, Swaminathan S, Karplus M. J Comput Chem 1983;4:187–217.

21. Jorgensen WL, Maxwell DS, Tirado-Rives J. J Am Chem Soc 1996;118:11225–11236.
22. Damm W, Frontera A, Tirado-Rives J, Jorgensen WL. J Comput Chem 1997;18:1955–1970.
23. Kuttel M, Brady JW, Naidoo KJ. J Comput Chem 2002;23:1236–1243. [PubMed: 12210149]
24. Kirschner KN, Woods RJ. Proc Natl Acad Sci USA 2001;98:10541–10545. [PubMed: 11526221]
25. Basma M, Sundara S, Calgan D, Vernali T, Woods RJ. J Comput Chem 2001;22:1125–1137. [PubMed: 17882310]
26. Kirschner KN, Woods RJ. J Phys Chem A 2001;105:4150–4155. [PubMed: 16518456]
27. Yin DX, Mackerell AD. J Comput Chem 1998;19:334–348.
28. Kalé L, Skeel R, Bhandarkar M, Brunner R, Gursoy A, Krawetz N, Phillips J, Shinozaki A, Varadarajan K, Schulten K. J Comput Phys 1999;151:283–312.
29. Darden T, York D, Pedersen LG. J Chem Phys 1993;98:10089–10092.
30. Smith SB, Cui YJ, Bustamante C. Science 1996;271:795–799. [PubMed: 8628994]
31. Clausen-Schaumann H, Rief M, Tolksdorf C, Gaub HE. Biophys J 2000;78:1997–2007. [PubMed: 10733978]
32. Carrion-Vazquez M, Oberhauser AF, Fowler SB, Marszalek PE, Broedel SE, Clarke J, Fernandez JM. Proc Natl Acad Sci USA 1999;96:3694–3699. [PubMed: 10097099]
33. Pensak DA, French AD. Carbohydrate Research 1980;87:1–10.
34. French, AD.; Rowland, RS.; Allinger, NL. Computer Modeling of Carbohydrate Molecules. In: French, AD.; Brady, JW., editors. ACS Symposium Series. Am. Chem. Soc; Washington, DC: 1989. p. 120-140.
35. Lu Z, Nowak W, Lee G, Marszalek PE, Yang W. J Am Chem Soc 2004;126:9033–9041. [PubMed: 15264836]
36. Lee G, Nowak W, Jaroniec J, Zhang Q, Marszalek P. J Am Chem Soc 2004;126:6218–6219. [PubMed: 15149204]
37. Lee G, Nowak W, Jaroniec J, Zhang Q, Marszalek P. Biophys J 2004;87:1456–1465. [PubMed: 15345528]
38. Takahashi Y, Nishikawa S. Macromol 2003;36:8656–8661.
39. Banks, W.; Greenwood, CT. Starch and Its Components. Edinburgh University Press; Edinburgh, Scotland: 1975.
40. Rundle RE. J Am Chem Soc 1947;69:1769–1772.
41. Booy FP, Chanzy H. Biopolymers 1979;18:2261–2266.
42. Thompson JC, Hamori E. Biopolymers 1969;8:689–694.

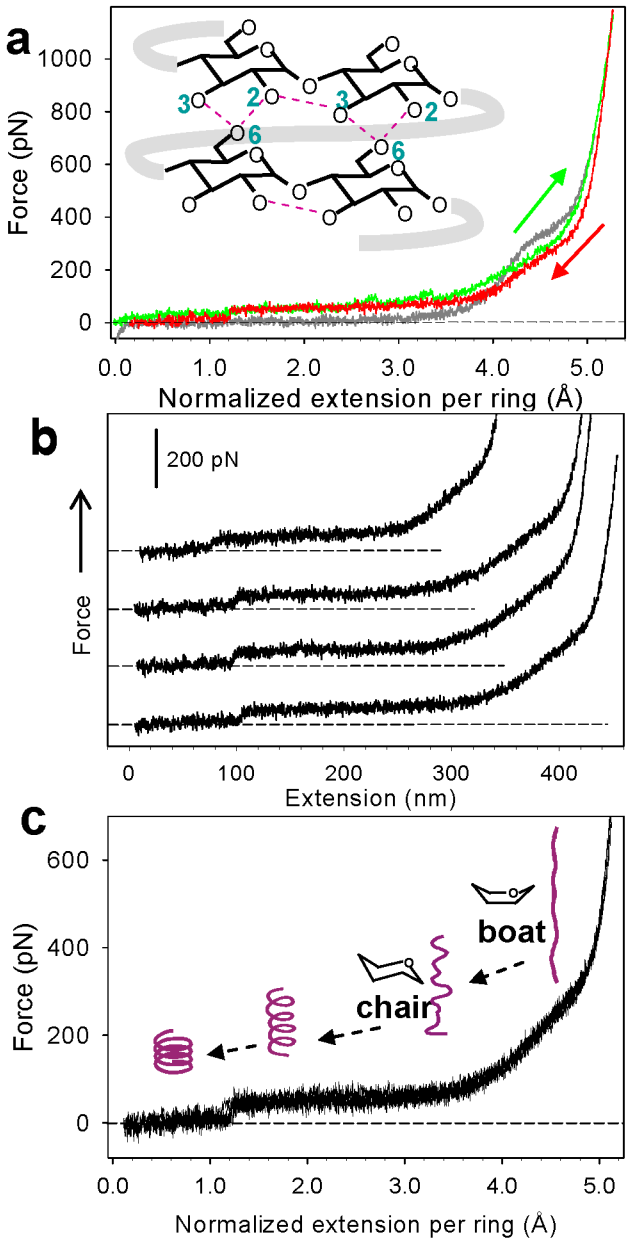

Figure 1.

AFM captures the formation of amylose helix in butanol. (a) Consecutive stretching (green curve) and relaxing force curves (red curve) of single amylose chains in butanol. The curve depicted in gray is a representative stretching curve of amylose in water. (*Inset*) Schematic structure of amylose helix showing inter-glucose hydrogen bond $O(3)_n$-$O(2)_{n+1}$ and the inter-turn hydrogen bonds $O(6)_n$-$O(2)_{n+6}$ and $O(6)_n$-$O(3)_{n+6}$. (b) Four relaxing force spectrograms of single amylose molecules of various lengths in butanol. (c) The four curves in (b) are normalized and superimposed. (*Inset*) A schematic illustration of amylose conformations during the relaxation process in butanol.

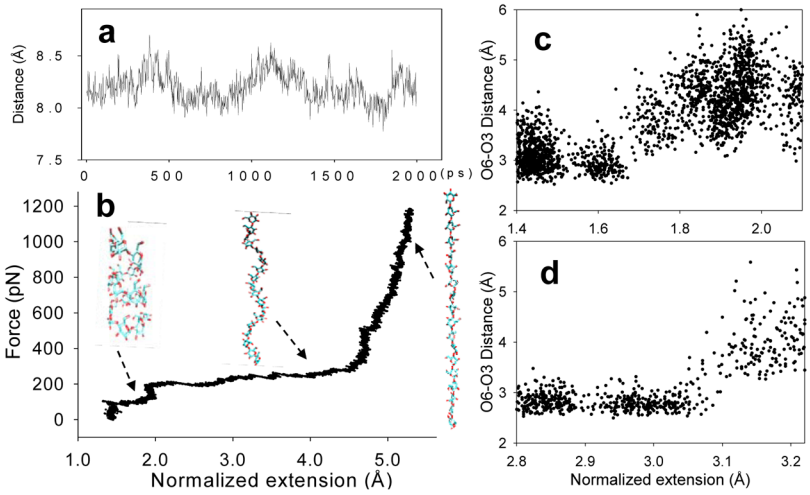

Figure 2.

SMD simulations of the stretching of amylose chains in explicit butanol reproduce AFM data. (a) Averaged distances between ring n and ring n+6 computed from the 2 ns equilibration trajectory. (b) The simulated force-extension curve for amylose in butanol. The inset shows snapshots of amylose structure at various phases of the stretching. (c) The distance between $O(2)_2$ and $O(6)_8$, plotted as a function of the normalized chain extension. (d) Similar to (c) but for the $O(3)_{10}$- $O(6)_{16}$ distance.

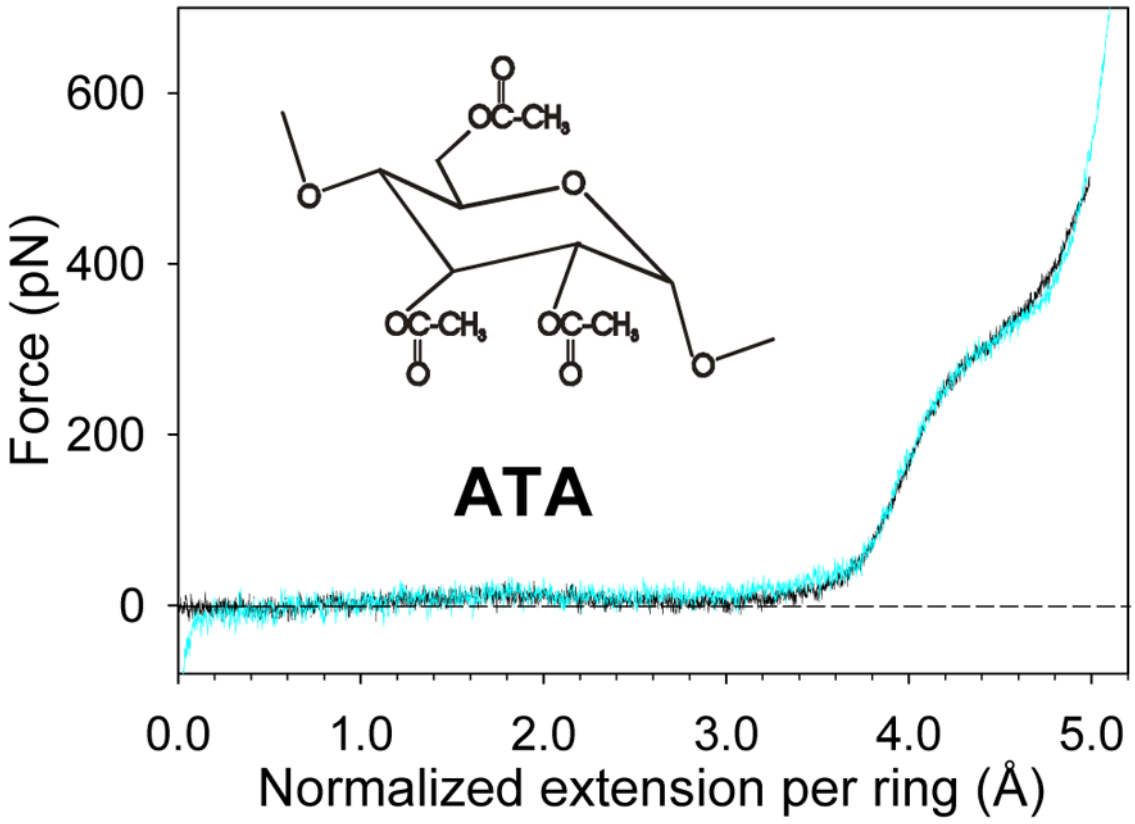

Figure 3.
Normalized force extension curves of single amylose triacetate (ATA) molecules in water (cyan) and in butanol (black). (*Inset*) ATA structure.

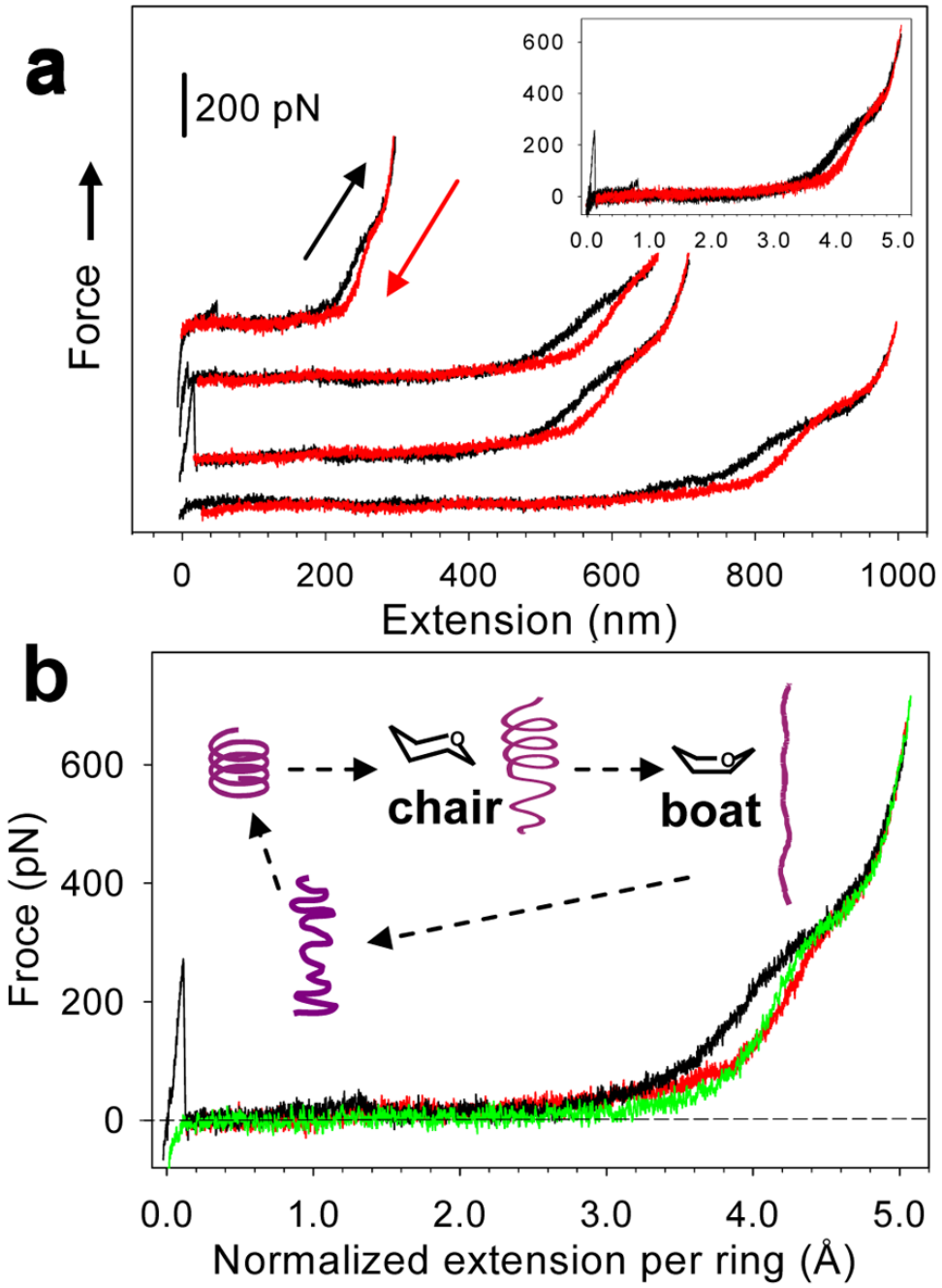

Figure 4.

Force spectroscopy captures the hysteretic elasticity of amylose in iodine solution. (a) Four pairs of consecutive stretching (black curves) and relaxing (red curves) force-extension curves of single amylose molecules of various lengths measured in aqueous iodine solution. (*Inset*) The same spectrograms superimposed after normalization. (b) A comparison of normalized consecutive stretching (black traces) and relaxing (red traces) force curves of amylose in aqueous iodine solution and a stretching force curve of amylose in water (green trace). (*Inset*) A schematic illustration of amylose conformations during stretching and relaxing processes.

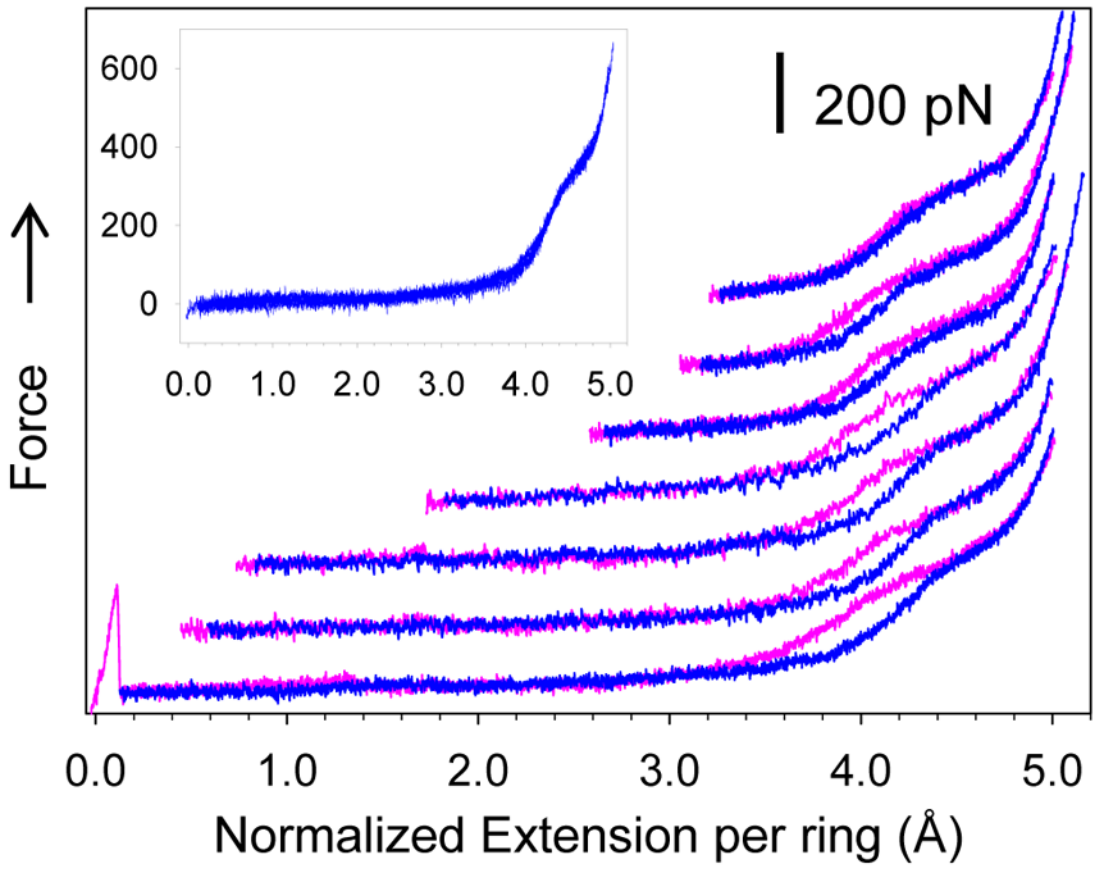

Figure 5.
A series of stretch-release force curves of single amylose molecules in iodine solution obtained after relaxing these molecules to different starting extensions. (*Inset*) The relaxing force curves for this series are normalized and superimposed.